Generating Haar-uniform Randomness using Quantum Stochastic Walks on a Photonic Chip

Authors[1, 2, 3, 4]

[1]*Center for Integrated Quantum Information Technologies (IQIT), School of Physics and Astronomy and State Key Laboratory of Advanced Optical Communication Systems and Networks, Shanghai Jiao Tong University, Shanghai 200240, China*

[2]*CAS Center for Excellence and Synergetic Innovation Center in Quantum Information and Quantum Physics, University of Science and Technology of China, Hefei, Anhui 230026, China*

[3]*Department of Physics and Astronomy, University of Florence, via G. Sansone 1, I-50019 Sesto Fiorentino (FI), Italy*

[4]*INFN Sezione di Firenze, via G. Sansone 1, I-50019 Sesto Fiorentino (FI), Italy**

As random operations for quantum systems are intensively used in various quantum information tasks, a trustworthy measure of the randomenss in quantum operations is highly demanded. Haar measure of randomness is a useful tool with wide applications such as boson sampling. A recent theoretical proposal was raised that combines quantum control theory and the driven many-body open quantum system model to generate Haar-uniform random operations. This opens up a promising route to converting classical randomness to quantum randomness, which, however, has never been experimentally demonstrated. Here, we implement two-dimensional quantum stochastic walk on the integrated photonic chip and demonstrate the average of all distribution profiles converges to the even distribution when the evolution length increases, suggesting the 1-pad Haar-uniform randomness. We further show that our two-dimensional array outperforms the one-dimensional array of the same number of waveguide for the speed of convergence. Our work demonstrates a highly scalable way to generate Haar-uniform randomness that can be useful building blocks to boost future quantum information techniques.

Random operation for quantum systems[1] plays an important role for a large variety of tasks in quantum information processing. Especially, as various studies on boson sampling[2–6] to demonstrate quantum computational supremacy[7,8] emerge in recent years, the Haar random unitary matrices[9] required for these studies have drawn ever increasing attention. The Haar measure of randomness is now investigated as more than a theoretical tool, but also the useful building block for quantum protocols or algorithms, with wide applications covering boson sampling[2–6], quantum cryptography[10], quantum process tomography[11], entanglement generation[12], fidelity estimation[13], and etc, which, therefore, motivate a series of efforts to raise experimental schemes on implementing random or pseudorandom quantum operations[14–16]. So far, these experimental schemes decompose random unitary matrix either by using a large number of quantum gates[14–16], or using photonic beamsplitters and interferometers[17,18] via Reck/Clements decomposition method[19,20], both of a considerably high complexity.

On the other hand, an alternative approach to generate Haar uniform random operations using quantum stochastic walks has been recently raised[21]. The rationale is based on quantum control theory that uses random classical pulses to control a quantum system, and the theory of driven many-body open quantum systems with stochastic dynamics. Instead of using quantum circuits or the programmable photonic networks with beam splitters and phase shifters, this scheme via continuous-time quantum stochastic walks[22] could be much more scalable, and beneficial for practical quantum experiments including larger-scale boson sampling. However, up to now, this scheme has never been demonstrated in experiments.

Photonic lattice is an ideal physical platform to implement continuous-time quantum walk, and a large evolution space in the photonic lattice allowing for real spatial two-dimensional quantum walks has been recently demonstrated[23,24]. While this physical system is suitable for coherent and pure quantum walk, the environmental decoherence term can also be intentionally introduced by lattice manipulation. The key process is to introduce classical randomness to the propagation constant along different sectors of each waveguide, which causes the randomness in the diagonal part of the Hamiltonian matrix. Therefore, quantum stochastic walks have been successfully demonstrated in the photonic lattice to simulate various open quantum systems[25,26].

In this work, we experimentally demonstrate the Haar-uniform randomness using quantum stochastic walks on the integrated photonic chips. We prepare samples of different random settings of propagation constant detunings and measure the light intensity distribution of quantum stochastic walks on these two-dimensional photonic evolution spaces. We demonstrate the average of all distribution profiles converges to the even distribution when the evolution length increases, suggesting the 1-pad Haar-uniform randomness. We further show that our two-dimensional array outperforms the one-dimensional array of the same number of waveguide for the speed of convergence. Our work demonstrates a highly scalable physical implementation for generating Haar-uniform randomness, which that can be useful building blocks to boost future quantum information techniques.

I. THE EXPERIMENTAL SCHEME

We start this section by briefly recalling the criterion of approximate q-designs[14,21,27] for an ensemle of unitary operators

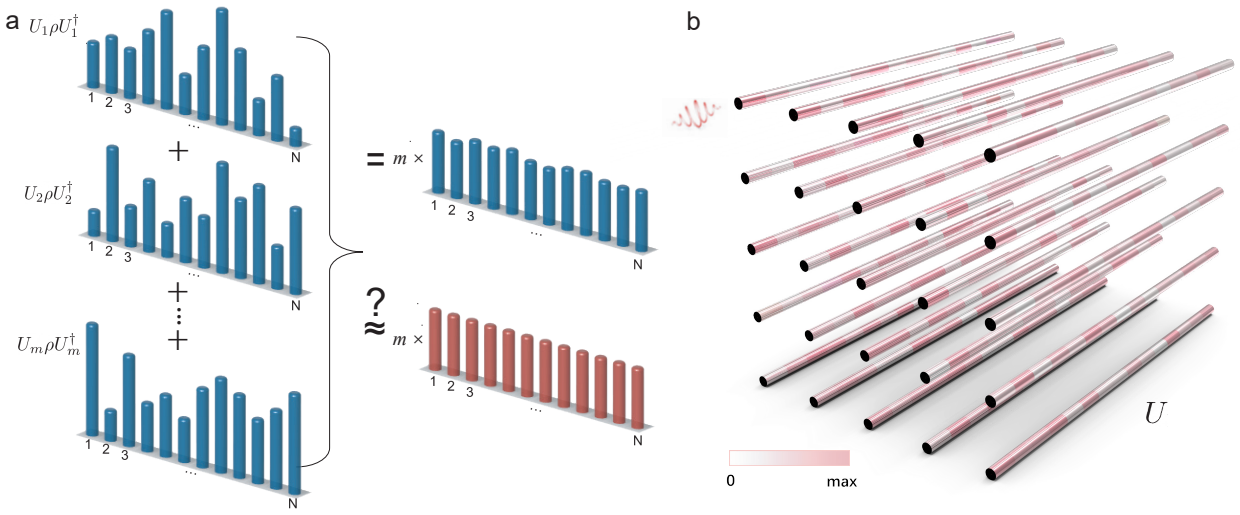

FIG. 1: **Generating Haar-uniform randomness using quantum stochastic walks.** (**a**) Illustration of averaging many quantum stochastic walks of a certain evolution time to reach the Haar-measure. The red columns represent the distribution of I/N appeared in Eq.(2). (**b**) Schematic diagram of introducing random delta beta detunings to implement quantum stochastic walks on the photonic chip. The colorbar shows the detuning strength of the propagation constant, where 'max' corresponds to the given $\Delta\beta$ amplitude. Photons are injected into one waveguide, and the evolution in the lattice corresponds to a unitary operation.

$\{U_i\}$ to meet the Haar measure:

$$\|\mathbb{E}_U[U_i^{\otimes q}\rho U_i^{\otimes q\dagger}] - \int_U U^{\otimes q}\rho U^{\otimes q\dagger}dU\|_\diamond < \varepsilon \qquad (1)$$

where $\|T\|_\diamond$ is the diamond norm of a superoperator T, ρ is the density matrix and ε is a considerably small value. $\mathbb{E}_U$ denotes the expected value, *i.e.*, the average of distribution for the ensemble of unitary operators. The second part is the result of distribution when unitaries follow the Haar measure.

For $q = 1$, the second part reduces to I/N, where N is the size of the unitary matrix U_i, and I is the identity matrix of the same size. Therefore, Eq.(1) becomes:

$$\|\mathbb{E}_U[U_i\rho U_i^\dagger] - I/N\| < \varepsilon \qquad (2)$$

This is inspiring from the experimental perspective. For any continous-time quantum evolution, it inherentally implements an unitary operation, *i.e.* $U\rho U^\dagger$. However, not all unitary operators could satisfy Eq.(2). Pure quantum walks, for instance, have a fixed ballistic distribution rather than even distribution. On the other hand, the theoretical proposal[21] shows that continous-time quantum stochastic walk could successfully reach the Haar measure after a certain evolution time.

Consider a photonic lattice where each waveguide is equally devided into the same number of segments, and each segment has a constant detuning of the propagation constant, with random detunings in all segments following a uniform distribution (See Fig.1b). The photon evolution through such a lattic with N waveguides just corresponds to the operation with U of a size N. The evolution can be described by an effective piecewise Hamiltonian H_{eff}. For each segment k, there is:

$$H_{\text{eff}}(k) = \sum_i^N(\beta_i + \Delta\beta_i(k))a_i^\dagger a_i + \sum_{j\neq i}^N C_{ij}(a_i^\dagger a_j + a_j^\dagger a_i) \qquad (3)$$

where β_i and C_{ij} are respectively the propagation constant and coupling coefficient for the lattice without any detunings. In practice, β_i is always set as the same for all waveguides. $\Delta\beta_i(k)$ is the constant detuning of the propagation constant for waveguide i at segment k, which can be experimentally achieved by tuning the writing speed (See details for $\Delta\beta$ tuning in Methods). The introduction of $\Delta\beta$ in H_{eff} has an effect of adding some classical dephasing terms in the diagonal part of density matrix.

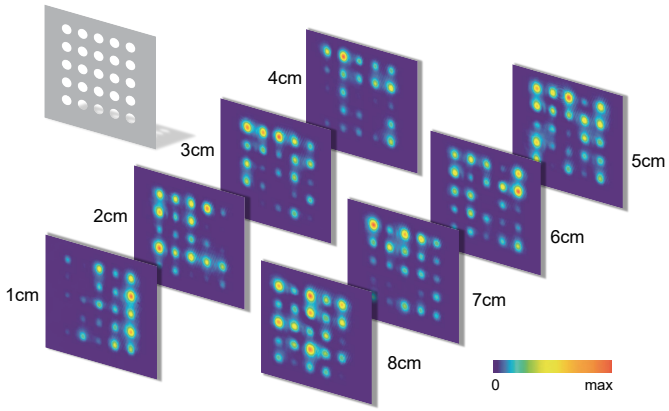

FIG. 2: **Experimental results for quantum stochastic walks.** The photonic evolution patterns of different evolution lengths for one random setting of photonic lattice. The corresponding evolution length of each graph is marked beside the graph. The mask illustrates how we read the figure data to get the probability distribution, with details explained in Methods.

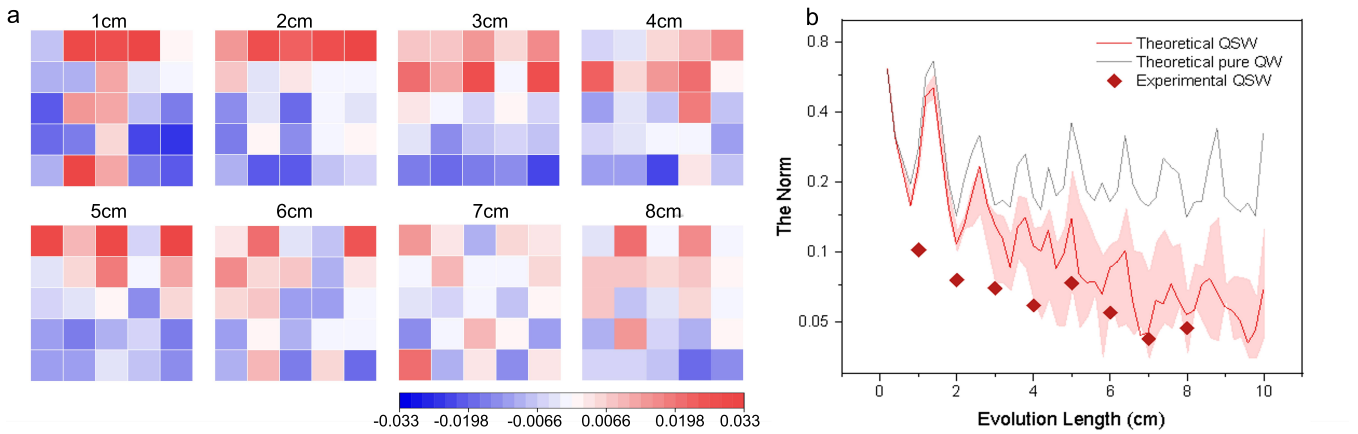

FIG. 3: **Convergence to the Haar measure.** (**a**) The heatmaps that show all elements of the matrix M for different evolution lengths. The matrix M for each evolution length is obtained by subtracting the matrix for equal distribution from the average distribution of 17 random settings of the same evolution length. The corresponding evolution length for each heatmap is listed above the heatmap. Note that a few elements have a value above 0.33 or below -0.33. They are represented in the heatmap using the color for 0.33 or -0.33, respectively. (**b**) The L2 norm $||M||$ for samples of different evolution lengths. QSW and QW stand for quantum stochastic walk and quantum walk, respectively. The theoretical results are obtained by setting Δz of 2mm and averaging 17 random settings, which are consistent with the experiment. Consider the potential error in reaching the precise $\Delta\beta$ amplitude in experiment, we add a shadow area with its upper and down edge corresponding to the result with a $\Delta\beta$ amplitude of 0.3mm^{-1} and 0.5mm^{-1}, respectively.

We use Ψ to denote the vector for wavefunction. It has a solution $\Psi(z) = (\prod_k e^{-iH_{\text{eff}}(k)\Delta z})\Psi(0)$ knowing the intitial wavefunction $\Psi(0)$, where Δz is the length of each segment. $|\Psi|^2$ yields the probability distribution, which can be straightforwardly measured in experiments. The probability distribution is exactly what we expect from the unitary operation $U\rho U^\dagger$.

In experiment, we prepare photonic lattices of 5×5 waveguides, a total evolution length of 8cm, and a segment length Δz of 2mm. The random $\Delta\beta$ detunings in all segments follow a uniform distribution under a $\Delta\beta$ amplitude of 0.4mm^{-1} (See details for waveguide preparation in Methods). We totally have 17 random settings for the detuning profiles. We inject photons from one waveguide of the lattice and measure the evolution patterns for an evolution length of 1cm, 2cm, 3cm, 4cm, 5cm, 6cm, 7cm, and 8cm, which will allow us to see how the performance changes with the evolution length.

II. RESULT ANALYSIS

As shown in Fig.2, we measure the photonic evolution pattern for different evolution lengths after injecting photon in the lattice of one random setting. We then read the intensity probability at each waveguide for each figure (See details in Methods). We have processed all 17 random settings and each has 8 different evolution lengths.

For each evolution length, we average the probability distribution of the 17 settings. What we obtain is the diagonal part of $\mathbb{E}_U[U_i\rho U_i^\dagger]$ in Eq.(2). The diagonal part of the other term in Eq.(2), I/N, can be viewed as the equal distribution at all 5×5 waveguides, which means each waveguide has an equal probability of 0.04. We substract 0.04 from each element of the measured average probability distribution matrix, and we can get the diagonal part of $\mathbb{E}_U[U_i\rho U_i^\dagger] - I/N$, which is a 25×1 vector and can be written in a 5×5 matrix M.

We use the heatmap to list the value of each element in the matrix M (See Fig.3a-h). Clearly, for a small evolution length, the fluctation around zero for these element values is much more fiece than that for a larger evolution length. We calculate the L2 norm of M, *i.e.*, $||M||$. If all elements in M are zero, $||M||$ will certainly be zero, while large deviations from zero in these elements make $||M||$ big. The calculated $||M||$ shown in Fig.3 well supports the results in heatmaps. $||M||$ gradually converges to a considerably small value when the evolution length increases. It matches the theoretical quantum stochastic walk results that dynamically decays to zero. As a comparison, the pure quantum walk always keeps a high norm value and does not show a sign of convergence. We further show in the Appendix A that convergence can theoretically be further improved when in increasing the number of samples, the $\Delta\beta$ amplitude, and the evolution length.

Our experiment demonstrates that the diagonal elements of $\mathbb{E}_U[U_i\rho U_i^\dagger]$ indeed go to uniform distribution. For the off-diagonal elements of $\mathbb{E}_U[U_i\rho U_i^\dagger]$, the experiment would be too complex and hence we have to rely on a theoretical argument. As seen in Appendix B, the most important result is Eq.(A6) that links the theoretical norm of $\mathbb{E}_U[U_i\rho U_i^\dagger] - I/N$ to our experimentally measured norm for M, namely the distance between the diagonal elements and the uniform distribution (denoted as D_d). There is another term in Eq.(A6) due to the off-diagonal part D_{od}. Although the experimental verification of D_{od} approaching to 0 for large m is complex, this theoretical conjecture has been analyzed. See more derivation in Appendix B. With both our experiment demonstration of diagonal part and the theoretical anlaysis of the diagonal part, we show that quantum stochastic walks can reach a 1-design

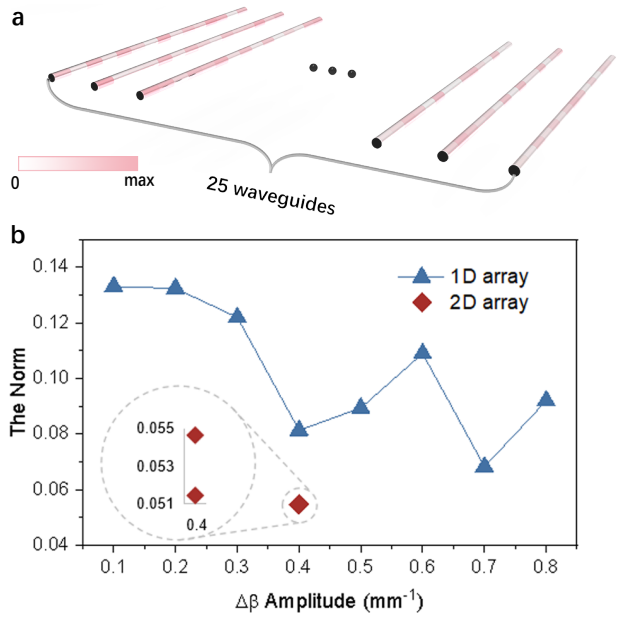

FIG. 4: **Compare the performance in one- and two-dimensional array.** (**a**) Schematic diagram of the one-dimensional photonic lattice of 25 waveguides with random tunings of the propagation constant. (**b**) The calculated L2 norm $\|M\|$ for one-dimensional (1D) and two-dimensional (2D) arrays. For two-dimensional array, we get two sets of norm values, each by averaging 6 random settings separately.

Haar measure at a long enough evolution length.

We further investigate the one-dimensional photonic lattice of 1×25 waveguides (see Fig.4a) and an evolution length of 8cm, while Δz is the same with the above two-dimensional lattice. We set eight different $\Delta\beta$ amplitudes, namely, 0.1, 0.2, 0.3, 0.4, 0.5, 0.6, 0.7 and 0.8 mm^{-1}, and each has 6 random settings. We average the 6 probability distributions for each $\Delta\beta$ amplitude and plot their $\|M\|$ in Fig.4b. As a comparison, we also show the diamond norm for two-dimensional array by averaging 6 random settings.

For the one-dimensional array, as $\Delta\beta$ amplitude increases, there is a slightly reducing trend of the norm. This is because a stronger dephasing effect caused by larger $\Delta\beta$s can facilitate a faster convergence to the Haar measure. However, even the norm for samples of 0.8mm^{-1} still far exceeds the norm for the two-dimensional samples with a $\Delta\beta$ amplitude of 0.4mm^{-1}. The two-dimensional quantum walk has demonstrated the same ballistic transport with the one-dimensional quantum walk, and yet a faster decay from the injection site than the latter, owing to much richer evolution paths[23]. The two-dimensional evolution space has also allowed for more flexible constructions of the Hamiltonian matrix[24]. In this work, we show that the two-dimensional quantum stochastic walk has a clear advantage in fast convergence to the Haar measure utilizing the rich evolution paths.

III. DISCUSSION

In all, we have experimentally implemented the theoretical proposal of generating Haar-uniform randomness using continuous-time quantum stochastic walks. By taking full advantages of large-scale integrated photonic chips and precise lattice manipulation techniques, we achieve two-dimensional continuous-time walks with random detunings in the propagation constant of waveguides. Therefore, we are able to demonstrate quantum stochastic walks on the photonic chips, and suggest the convergence to Haar-uniform randomness at a large evolution length. We further show the faster convergence using two-dimensional quantum stochastic walks than the one-dimensional ones.

We have successfully demonstrated the usage of the classical randomness (*i.e.*, the random settings of delta beta detunings) to make the unitary 1-design distribution as an important source for quantum randomness. The convergence can be further improved with larger delta beta detunings, more samples of different delta beta detunings and a longer evolution time. This method offers a highly feasible alternative to the quantum gate approach or the Reck/Clements decomposition approach for generating Haar randomness. This utilization of two-dimensional continuous-time quantum stochastic walk on photonic chips sheds light for more applications that need Haar randomness and it's worthy of further investigation.

Methods

Delta beta approach. We measure $\Delta\beta$ using the directional coupler approach. One of the waveguide is written using a speed $V_0 = 5$ mm/s, and the other waveguide using a different speed V ($V - V_0 = \Delta V$) that will lead to a detuned propagation constant $\Delta\beta$ on this waveguide. In the detuned directional coupler, the effective coupling coefficient C_{eff} can be obtained using the same coupling mode method as that for the normal directional coupler[28], but C_{eff} contains the detuning effect from $\Delta\beta$ through this equation[29]: $C_{\text{eff}} = \sqrt{(\Delta\beta/2)^2 + C^2}$, where C is the coupling coefficient for a normal directional coupler. Therefore, $\Delta\beta$ can be calculated when C_{eff} and C are both characterized. We then plot $\Delta\beta$ (unit: mm^{-1}) against ΔV (unit: mm/s), and fit it linearly: $\Delta\beta = 0.02 \times \Delta V$. Knowing this, we can randomly generate $\Delta\beta$ of $0.01 - 0.4$ mm^{-1} by varying ΔV between $0.5 - 20$ mm/s.

Waveguide preparation. For the 17 random settings, each has 8 different evolution lengths. As it is not convenient to measure the evolution patterns in the middle of the waveguide, we have to make 8 samples with a length of 1cm, 2cm, ..., 8cm, respectively. We have ensured the 8 samples follow the same random setting, for instance, $\Delta\beta$ profiles for the 4-cm-long sample are exactly the same with those in the first 4cm of the 8-cm-long sample. All the waveguides are fabricated using the femtosecond laser direct writing technique[30–32]. We direct a 513-nm femtosecond laser (up converted from a pump laser of 10W, 1026nm, 290fs pulse duration, 1 MHz repetition rate) into a spatial light modulator (SLM) to shape the laser pulse in the temporal and spatial domain. The writing speed

is precisely controlled for each segment to ensure the introduction of the target $\Delta\beta$ value. We then focus the pulse onto a pure borosilicate substrate with a 50X objective lens (numerical aperture: 0.55). Power and SLM compensation were processed to ensure the waveguide uniformity.

Measure probability distribution from graphs. When collecting the data from experiments, we obtained the corresponding ASCII file, which is essentially a matrix of pixels. We created a 'mask' containing the pixel coordinate of the circle centre and the radius in pixels for each waveguide, and summed the light intensity for all the pixels within each circle using Matlab. The normalized proportion of light intensity for each circle represents the probability at the corresponding waveguide.

Acknowledgments

The authors thank Jian-Wei Pan for helpful discussions. This research was supported by National Key R&D Program of China (2019YFA0308700, 2017YFA0303700), National Natural Science Foundation of China (61734005, 11761141014, 11690033, 11904229), Science and Technology Commission of Shanghai Municipality (STCSM) (17JC1400403), and Shanghai Municipal Education Commission (SMEC) (2017-01-07-00-02- E00049). X.-M.J. acknowledges additional support from a Shanghai talent program.

Author Contributions. To be filled. **Competing Interests.** The authors declare no competing interests. **Data Availability.** The data that support the plots within this paper and other findings of this study are available from the corresponding author upon reasonable request.

* Electronic address: xianmin.jin@sjtu.edu.cn

1. Guhr, T., Müller-Groeling, A., & Weidenmüller, H. A. Random-Matrix Theories in Quantum Physics: Common Concepts. *Phys. Rep.* **299**, 189-425 (1998).
2. Spring, J. B., Metcalf, B. J., Humphreys, P. C., Kolthammer, W. S., Jin, X. M., Barbieri, M., Datta, A., Thomas-Peter, N., Langford, N. K., Kundys, D., Gates, J. C., Smith, B. J., Smith, P. G. R., & Walmsley, I. A. Boson sampling on a photonic chip. *Science* **339**, 798-801 (2013).
3. Broome, M.A., Fedrizzi, A., Rahimi-Keshari, S., Dove, J., Aaronson, S., Ralph, T. C., & White, A. G. Photonic boson sampling in a tunable circuit. *Science* **339**, 794-798 (2013).
4. Tillmann, M., Dakić, B., Heilmann, R., Nolte, S., Szameit, A., & Walther, P. Experimental boson sampling. *Nat. Photon.* **7**, 540-544 (2013).
5. Spagnolo, N., Vitelli, C., Bentivegna, M., Brod, D. J., Crespi, A., Flamini, F., Giacomini, S., Milani, G., Ramponi, R., Mataloni, P., Osellame, R., Galvão, E. F., & Sciarrino, F. Experimental validation of photonic boson sampling. *Nat. Photon.* **8**, 615-620 (2014).
6. Wang, H., He, Y., Li, Y. H., Su, Z. E., Li, B., Huang, H. L., Ding, X., Chen, M. C., Liu, C., Qin, J., Li, J. P., He, Y. M., Schneider, C., Kamp, M., Peng, C. Z., Höfling, S., Lu, C. Y. & Pan, J. W. High-efficiency multiphoton boson sampling. *Nat. Photon.* **11**, 361-365 (2017).
7. Harrow, A. W., & Montanaro, A. Quantum computational supremacy. *Nature* **549**, 203-209 (2017).
8. Wu, J., Liu, Y., Zhang, B., Jin, X., Wang, Y., Wang, H., & Yang, X. A benchmark test of boson sampling on Tianhe-2 supercomputer. *Nat. Sci. Rev.* **5**, 715-720 (2018).
9. Zyczkowski,K. & Kuś, M. Random unitary matrices. *J. Phys. A: Math. Gen.* **27**, 4235-4245 (1994).
10. Hayden, P., Leung, D., Shor, P. W., & Winter, A. Randomizing Quantum States: Constructions and Applications. *Commun. Math. Phys.* **250**, 371 (2004).
11. Bendersky, A., Pastawski, F., & Paz, J. P. Selective and Efficient Estimation of Parameters for Quantum Process Tomography. *Phys. Rev. Lett.* **100**, 190403 (2008).
12. Hamma, A., Santra, S., & Zanardi, P. Quantum Entanglement in Random Physical States. *Phys. Rev. Lett.* **109**, 040502 (2012).
13. Dankert, C., Cleve, R., Emerson, J., & Livine, E. Exact and Approximate Unitary 2-Designs and Their Application to Fidelity Estimation. *Phys. Rev. A* **80**, 012304 (2009).
14. Harrow, A. W., & Low, R. A. Random quantum circuits are approximate 2-designs. *Commun. Math. Phys.* **291**, 257-302 (2009).
15. Emerson, J., Weinstein, Y. S., Saraceno, M., Lloyd, S., & Cory, D. G. Pseudo-Random Unitary Operators for Quantum Information Processing. *Science* **302**, 2098-2100 (2003).
16. Alexander, R. N., Turner, P. S., & Bartlett, S. D. Randomized Benchmarking in Measurement-Based Quantum Computing. *Phys. Rev. A* **94**, 032303 (2016).
17. Russell, N. J., Chakhmakhchyan, L., O'Brien, J. L., & Laing, A. Direct dialling of Haar random unitary matrices. *New J. Phys.* **19**, 033007 (2017).
18. Burgwal,R., Clements, W. R., Smith, D. H., Gates, J. C., Steven Kolthammer, W., Renema, J. J., & Walmsley, I. A. Using an imperfect photonic network to implement random unitaries. *Opt. Express* **25**, 28236-28245 (2017).
19. Reck, M., Zeilinger, A., Bernstein, H. J., & Bertani, P. Experimental realization of any discrete unitary operator. *Phys. Rev. Lett.* **73**, 58-61 (1994).
20. Clements, W. R., Humphreys, P. C., Metcalf, B. J., Kolthammer, W. S., & Walmsley, I. A. Optimal design for universal multiport interferometers. *Optica* **3**, 1460-1465 (2016).
21. Banchi,L., Burgarth D. & Kastoryano, M. J. Driven Quantum Dynamics: Will It Blend? *Phys. Rev. X* **7**, 041015 (2017).
22. Whitfield, J. D., Rodríguez-Rosario, C. A., & Aspuru-Guzik, A. Quantum stochastic walks: A generalization of classical random walks and quantum walks. *Phys. Rev. A* **81**, 022323 (2010).
23. Tang, H., Lin, X. F., Feng, Z., Chen, J. Y., Gao, J., Sun, K., Wang, C. Y., Lai, P. C., Xu, X. Y., Wang, Y., Qiao, L. F., Yang, A. L., & Jin, X., M. Experimental Two-dimensional Quantum Walk on a Photonic Chip. *Sci. Adv.* **4**, eaat3174 (2018).
24. Tang, H., Di Franco, C., Shi, Z. Y., He, T. S., Feng, Z., Gao, J., Li, Z. M., Jiao Z. Q., Wang, T. Y., Kim, M. S.,& Jin, X. M. Experimental quantum fast hitting on hexagonal graphs. *Nat. Photon.*

12, 754-758 (2018).
25. Caruso, F., Crespi, A., Ciriolo, A. G., Sciarrino, F., & Osellame, R. Fast escape of a quantum walker from an integrated photonic maze. *Nat. Commun.* **7**, 11682 (2016).
26. Tang, H., Feng, Z., Wang, Y. H., Lai, P. C., Wang, C. Y., Ye, Z. Y., Wang, C. K., Shi, Z. Y., Wang, T. Y., Chen, Y., Gao, J. & Jin, X., M. Experimental quantum stochastic walks simulating associative memory of Hopfield neural networks. *Phys. Rev. Applied* **11**, 024020 (2019).
27. Brandão, F. G. S. L., Harrow, A. W., & Horodecki, M. Local Random Quantum Circuits Are Approximate Polynomial-Designs. *Commun. Math. Phys.* **346**, 397–434 (2016).
28. Szameit, A., Dreisow, F., Pertsch, T., Nolte, S.,& Trnnermann, A. Control of directional evanescent coupling in fs laser written waveguides. *Opt. Express* **15**, 1579-1587 (2007).
29. Lebugle, M., Gräfe, M., Heilmann, R., Perez-Leija, A., Nolte, S., & Szameit, A. Experimental observation of n00n state bloch oscillations. *Nat. Commun.* **6**, 8273 (2015).
30. Crespi, A., Osellame, R., Ramponi, R., Brod, D. J., Galvão, E. F., Spagnolo, N., Vitelli, C., Maiorino, E., Mataloni, P., & Sciarrino, F. Integrated multimode interferometers with arbitrary designs for photonic boson sampling. *Nat. Photon.* **7**, 545-549 (2013).
31. Chaboyer, Z., Meany, T., Helt, L. G., Withford, M. J., & Steel, M. J. Tunable quantum interference in a 3D integrated circuit. *Sci. Rep.* **5**, 9601 (2015).
32. Feng, Z., Wu, B. H., Zhao, Y. X., Gao, J., Qiao, L. F., Yang, A. L., Lin, X. F., & Jin, X. M. Invisibility Cloak Printed on a Photonic Chip. *Sci. Rep.* **6**, 28527 (2016).

-

Appendix A: The $\Delta\beta$ photonic approach for a long evolution length

As shown in Fig. A1, for a longer evolution length, with a $\Delta\beta$ amplitude of around 0.3 -0.5 mm^{-1}, the norm of M becomes very close to zero. This suggests that the diagonal part of $\mathbb{E}_U[U_i\rho U_i^\dagger]$ can go to uniform distribution for a long evolution of quantum stochastic walk.

Appendix B: Remarks on the convergence towards the completely mixing evolution

As discussed in the main text, for $q = 1$ we may formally study convergence towards a fully mixing evolution via the diamond distance $\|\mathcal{E}_{\text{ensemble}} - \mathcal{E}_{\text{Haar}}\|_\diamond$ between the quantum channel that mathematically describes the average over m discrete unitaries, $\mathcal{E}_{\text{ensemble}}[\rho] = \sum_{j=1}^m U_j\rho U_j^\dagger$, and the quantum channel that describes continuous averages over Haar-random unitaries $\mathcal{E}_{\text{Haar}}[\rho] = \int dU\, U\rho U^\dagger$. Such distance can be written as (see *e.g.* Ref.[A1])

$$\|\mathcal{E}_{\text{ensemble}} - \mathcal{E}_{\text{Haar}}\|_\diamond = \max_\Psi \|(\mathbb{1}\otimes\mathcal{E}_{\text{ensemble}} - \mathbb{1}\otimes\mathcal{E}_{\text{Haar}})(\Psi)\|_1 \tag{A1}$$

where the maximization is over quantum states $\Psi = |\Psi\rangle\langle\Psi|$. Although such maximization can be efficiently solved using semidefinite programming for small dimensional Hilbert spaces, it is generally complex to estimate the diamond distance from measurement data. Therefore, we study simpler quantities that are related to the diamond distance via bounds.

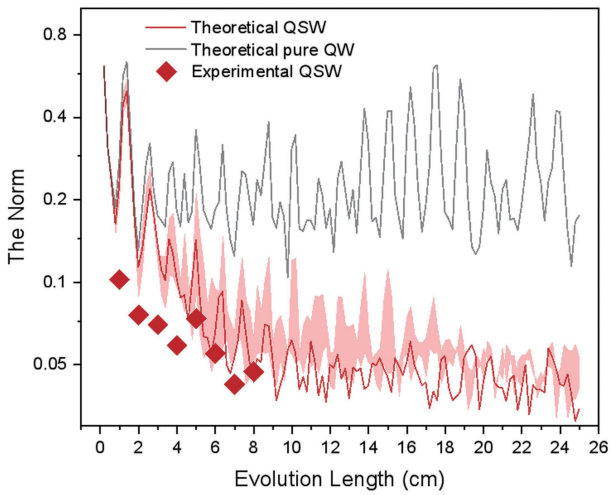

FIG. A1: **Convergence to the uniform distribution.** The L2 norm $\|M\|$ for samples of different evolution lengths. The theoretical results are obtained using the same setting with that in in Fig. 2. The curve for QSW corresponds to a $\Delta\beta$ amplitude of 0.4mm^{-1}. The shadow area with its upper and down edge correspond to the result with a $\Delta\beta$ amplitude of 0.3mm^{-1} and 0.5mm^{-1}, respectively.

We first recall one of the possible definitions of the trace norm (see *e.g.* Ref. [A2] Theorem 13.2)

$$\|\rho - \sigma\|_1 = \max_E \sum_i |\,\text{Tr}[E_i(\rho - \sigma)]|, \tag{A2}$$

where the maximum is taken over all possible POVMs such that $\sum_i E_i = \mathbb{1}$. With the above definition, we may introduce the following inequality

$$\|\mathcal{E}_{\text{ensemble}} - \mathcal{E}_{\text{Haar}}\|_\diamond \leq N\|\chi_{\text{ensemble}} - \chi_{\text{Haar}}\|_1\,, \tag{A3}$$

where $\chi_t = \mathbb{1}\otimes\mathcal{E}_t[|\Phi\rangle\langle\Phi|]$ is the Choi-Jamiołkowski state associated to the channel $\mathcal{E}_t$ and $|\Phi\rangle = \sum_{j=1}^N |jj\rangle/N$. Indeed, using (A2) in (A1) we may write for two generic channels, $\mathcal{E}_0$ and $\mathcal{E}_1$, the following inequality (also discussed in Ref. [A1] Exercise 3.6)

$$\begin{aligned}
\|\mathcal{E}_0 - \mathcal{E}_1\|_\diamond &= \max_\Psi \|(\mathbb{1}\otimes\mathcal{E}_0 - \mathbb{1}\otimes\mathcal{E}_1)(\Psi)\|_1 \\
&= \max_{E,\Psi} \sum_i |\,\text{Tr}\,[E_i(\mathbb{1}\otimes\mathcal{E}_0 - \mathbb{1}\otimes\mathcal{E}_1)(\Psi)]\,| \\
&= \max_{E,M} \sum_i |\,\text{Tr}\left[E_i(M\otimes\mathbb{1})(\chi_0 - \chi_1)M^\dagger\otimes\mathbb{1}\right]| \\
&= \max_M \|(M\otimes\mathbb{1})(\chi_0 - \chi_1)M^\dagger\otimes\mathbb{1}\|_1 \\
&\leq \max_M \|M\|_\infty^2\|\chi_0 - \chi_1\|_1 \\
&\leq \max_M \|M\|_2^2\|\chi_0 - \chi_1\|_1 \\
&= N\|\chi_0 - \chi_1\|_1,
\end{aligned}$$

where, without loss of generality, we have set $|\Psi\rangle = M \otimes \mathbb{1} |\Phi\rangle$, so that M satisfies $\|M\|_2^2 = \mathrm{Tr}\, M^\dagger M = N$ due to normalization. Indeed, from $|\Psi\rangle = \sum_{ij} \Psi_{ij} |ij\rangle$ we may set $M_{ij} = \sqrt{N}\Psi_{ij}$. In the fifth line we use the property $\|ABC\|_1 \leq \|A\|_\infty \|B\|_1 \|C\|_\infty$ (see Ref[A1] section 2.3.1), and in sixth line $\|A\|_\infty \leq \|A\|_2$.

The trace distance in Eq. (A3) could be measured experimentally as follows. The state χ_{ensemble} may be created by first generating path-entangled photonic states, and then sending half of the entangled state inside the linear-optical network that implements a quantum walk (or any other unitary). On the other hand, using simple properties of Haar integrals we find $\chi_{\text{Haar}} = \mathbb{1}/N^2$. The resulting experiment, although technically possible, is made more challenging by the use of entangled photon sources and by the demand of complete tomography, for reconstructing χ_{ensemble}. In order to introduce a simpler quantity for experiments we expand χ_{ensemble} into the basis $|i\rangle$, where $|i\rangle$ means that a photon is injected (or detected) in the ith waveguide. Using the definition of the Choi-Jamiołkowski state, we may write

$$\chi_{\text{ensemble}} = \sum_{ij,kl} \frac{1}{N} \langle k| \mathcal{E}_{\text{ensemble}}[|i\rangle\langle j|]\, |l\rangle \;\; |ik\rangle\langle kl| = \\ = \sum_{ij,kl} \chi_{ik,jl} |ik\rangle\langle kl| \;, \tag{A4}$$

where we have defined $\chi_{ik,jl} = \langle k| \mathcal{E}_{\text{ensemble}}[|i\rangle\langle j|]\, |l\rangle /N$. We may now split

$$\chi_{\text{ensemble}} = \chi_{\text{d}} + \chi_{\text{od}}, \tag{A5}$$

where $\chi_{\text{d}} = \sum_{ik} \chi_{ik,ik} |ik\rangle\langle ik|$ is the diagonal part or χ_{ensemble} and χ_{od} its off-diagonal part. Therefor, using the bound (A3) and the triangle inequality we may write

$$\|\mathcal{E}_{\text{ensemble}} - \mathcal{E}_{\text{Haar}}\|_\diamond \leq N(D_{\text{d}} + D_{\text{od}}) \,, \tag{A6}$$

where D_{d} measures the distance of the diagonal elements from the uniform distribution,

$$D_{\text{d}} = \|\chi_d - \mathbb{1}/N^2\|_1 = \sum_{ik} \left| \chi_{ik,ik} - \frac{1}{N^2} \right| = \tag{A7}$$

$$= \sum_{ik} \frac{1}{N} \left| \sum_{l=1}^{m} \langle k| U_l |i\rangle\langle i| U_l^\dagger |k\rangle - \frac{1}{N} \right| = \tag{A8}$$

$$= \frac{1}{N} \sum_{i,k=1}^{N} \left| \sum_{l=1}^{m} |\langle k| U_l |i\rangle|^2 - \frac{1}{N} \right|, \tag{A9}$$

and $D_{\text{od}} = \|\chi_{\text{od}}\|_1 \leq 2$ measures the strengths of the off-diagonal elements. The quantity D_{d} is what we have experimentally measured, while to estimate D_{od} we need complex entangled inputs and off-diagonal measurements.

Supplementary Reference

[A1] Watrous,J. The theory of quantum information. *Cambridge University Press* (2018).
[A2] Bengtsson, I. & Zyczkowski, K. Geometry of quantum states: an introduction to quantum entanglement. *Cambridge University Press* (2017).